

# MICROMORPH n-i-p TANDEM CELLS WITH ASYMMETRIC INTERMEDIATE REFLECTORS

F.-J. Haug<sup>1</sup>, T. Söderström<sup>1,2</sup>, V. Terrazzoni-Daudrix<sup>1</sup>, C. Ballif<sup>1</sup>, H. Sai<sup>3</sup>, M. Kondo<sup>3</sup>

<sup>1</sup> Ecole Polytechnique Fédérale de Lausanne (EPFL), Photovoltaics and Thin Film Electronics Laboratory,  
Rue A.-L. Breguet 2, 2000 Neuchâtel, Switzerland

<sup>2</sup> now at University of New South Wales, School of Photovoltaic and Renewable Energy Engineering,  
Sydney, N.S.W. 2052, Australia

<sup>3</sup> National Institute of Advanced Industrial Science and Technology (AIST), Central 2,  
Umezono 1-1-1, Tsukuba, Ibaraki 305-5868, Japan

**ABSTRACT:** We present tandem thin film silicon solar cells in n-i-p configuration with 12% initial efficiency. The stabilized efficiency of these devices is 10%. This result is obtained by the combination of a microcrystalline bottom cell on randomly textured substrate and an asymmetric intermediate reflector that establishes a well adapted surface texture for the amorphous top cell. After successfully integrating these two steps, we obtain micromorph tandems cells with size of typically 0.25 cm<sup>2</sup>. The best cell among an array of 16 devices on the 4x4 cm<sup>2</sup> sample area showed an initial efficiency of 12% with an open circuit voltage of  $V_{oc} = 1.335$  V, a short circuit current density of  $j_{sc} = 12.1$  mA/cm<sup>2</sup> and a fill factor of  $FF = 74.2\%$ . After carrying out the 1000 h light soak, this particular cell stabilized at 1.320 V, 11.9 mA/cm<sup>2</sup>, 62.7%, giving a stable efficiency of 9.8%. We observed some variation in the stabilized FFs, an adjacent cell with FF of 65.7 yields a stable efficiency of 10.0%.  
**Keywords:** Thin film silicon, Flexible substrate, Multijunction solar cell

## 1 INTRODUCTION

Thin film silicon solar cells are commonly classified into p-i-n and n-i-p type which refers to their deposition sequence. Because illumination is always from the p-side, n-i-p cells are applicable to opaque substrates like flexible steel foils [1]; the p-i-n configuration is illuminated through the substrate which requires high transparency. This is naturally achieved on glass [2], and was recently also demonstrated for flexible polymers [3]. Flexible substrates have obvious advantages for deployment and building integration, and they are also attractive for low cost production; roll-to-roll processes require smaller system footprint and allow larger batch size (a reel may hold as much as a kilometer compared to glass plates not exceeding a few m<sup>2</sup>). Finally, the substrate itself should also contribute to low production cost, ideally consists of a low cost plastic material like poly-ethylene.

The latter aspect interferes with another requirement of thin film silicon solar cells, which is the necessity of light trapping. For both, amorphous and microcrystalline silicon, the absorption length of near-IR light exceeds the mean free path of charge carriers. Therefore, thin cells are preferable for efficient charge collection. Thin absorber films are equally desirable in terms of production throughput. Within this limitation, the effective light path inside a given film thickness can be prolonged by light scattering at textured interfaces [4]. In the p-i-n configuration, this is achieved by growing the transparent front contact under conditions that result in naturally textured surfaces [5, 6], or by additional etching steps after their deposition [7]. In the n-i-p configuration, texturing of the metal contact can be achieved by the formation of preferential surface facets [1], but the underlying crystallization process typically requires that the substrate is held at elevated temperature during deposition. This texturing process is thus limited to steel and polyimide substrates. On low cost substrates like poly-ethylene, the required texture must be incorporated

into the substrate itself, from there it carried into the metal contact and subsequent layers by conformal coverage. Texturing can be achieved either directly by hot embossing [8] or by embossing into a UV curable polymer [9, 10], using suitable master structures.

In this contribution, we report on the fabrication of tandem solar cells using a microcrystalline bottom cell on a randomly textured Asahi-U substrate covered with an Ag/ZnO reflector. After coverage with the 2 to 4  $\mu$ m thick bottom cell, the initially pyramidal texture is replaced with the typical, cauliflower-like surface morphology of microcrystalline silicon which is not suitable for light scattering in the top cell. We ameliorate this issue by applying an intermediate reflector layer that establishes a suitable growth template for the amorphous cell. This cell design yields an initial efficiency of 12% and results in a stabilized efficiency of 10%.

## 2 EXPERIMENTAL

For ease of handling, the development was carried out on rigid substrates, but all processing steps, foremost the substrate temperature, were kept compatible with a low cost plastic substrate (poly-ethylene-naphthalate (PEN),  $T_g = 120^\circ\text{C}$ ). The fabrication of the bottom cell has been described elsewhere [11], in short an Asahi-U substrate was covered with an Ag/ZnO bi-layer (200 nm + 40 nm) which serves as opaque back contact. The microcrystalline absorber layer was deposited at AIST by plasma enhanced chemical vapour deposition (PE-CVD) at 170°C, an rf-power density of 0.04 W/cm<sup>2</sup>, and a pressure of 2 mbar from a precursor gas mixture of 10.5 sccm of silane diluted in 380 sccm of hydrogen. Similar conditions were used for the deposition of the amorphous top cell [12], except that excitation frequency was in the VHF region at 70 MHz, and that the ratio between hydrogen and silane was two. The ZnO intermediate reflector, as well as the front contact, were deposited by low pressure chemical vapour deposition (LP-CVD),

using di-ethyl-zinc (DEZ) and water. The conductivity in LP-CVD ZnO films is adjusted by doping with di-borane ( $B_2H_6$ ), intermediate reflector and front contact consist of 1.8 and 5  $\mu\text{m}$  thick films, respectively. Further details on micromorph tandem cells with asymmetric intermediate reflector are found in ref. [13]. Typically 16 cells with an area of 0.25  $\text{cm}^2$  are structured on a 4x4  $\text{cm}^2$  plate. The  $V_{oc}$  and the FF are evaluated from a j-V measurement at 25°C under AM1.5 illumination from a dual source solar simulator (Wacom). The  $j_{sc}$  is determined independently by convoluting the AM1.5g spectrum with the EQEs of top and bottom cells which are measured under red and blue bias light, respectively. Finally, the efficiency is calculated using  $V_{oc}$ , FF and the limiting current density. This conservative procedure avoids uncertainties with the exact determination of the cell size.

### 3 RESULTS AND DISCUSSION

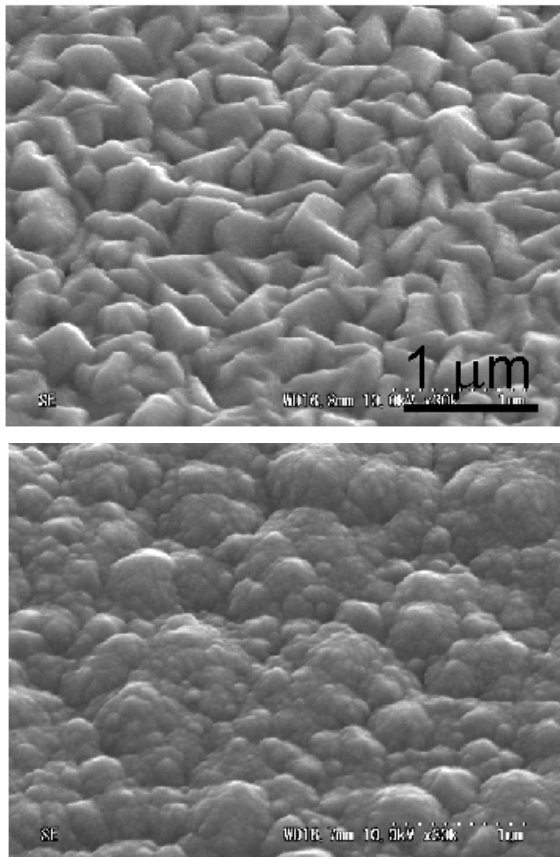


**Figure 1:** Surface morphology of the Asahi-U substrate covered with the Ag/ZnO reflector (top) and after deposition of a 4  $\mu\text{m}$  thick microcrystalline bottom cell (bottom) [14]. Image size approximately 4 x 3  $\mu\text{m}^2$ .

#### 3.1 Microcrystalline bottom cells

Figure 1 compares the morphology of the ZnO/Ag reflector on Asahi U substrate and the surface of a 4  $\mu\text{m}$  thick microcrystalline cell on top of this substrate. Both surfaces have comparable roughness of about 30 nm, but the pyramidal texture of the substrate is no longer distinguishable; instead the surface consists of the cauliflower-like texture which is typical for thick microcrystalline films. Compared to the substrate surface

the amount of light scattering from the cell surface is weak. Assuming that the comparatively thin top cell reproduces this roughness, light scattering is clearly not sufficient for high top cell current.

The design rule for current matching in micromorph tandem cells starts by looking at the current density that is generated by the bottom cell alone. Assuming similar blue response in the top cell, the current density generated by the bottom cell alone will simply be distributed within the two sub-cells. The microcrystalline cells in this investigation are 4  $\mu\text{m}$  thick and deliver close to 28  $\text{mA}/\text{cm}^2$  (using an ITO front contact that serves also as anti-reflection coating) [11]. Assuming that the recombination junction between the cells absorbs about 0.5  $\text{mA}/\text{cm}^2$ , the matched current density could be above 13  $\text{mA}/\text{cm}^2$ . Note that the impractically high bottom cell thickness of this experiment can be reduced by using more appropriate substrate textures [15].

#### 3.2 Amorphous top cells

When an amorphous cell is stacked on a microcrystalline one in a simple tandem design, the top cell essentially absorbs only a single pass of light because the microcrystalline cell underneath absorbs all light that is transmitted; there is no light trapping. This situation was long ago identified as bottleneck in micromorph cell design, and the use of an intermediate reflector layer was suggested as solution [16]. Compared to p-i-n cells where light scattering takes place at least once at the front interface, the situation is less favourable in n-i-p cells because whatever interface texture was present at the back reflector is flattened out by the bottom cell. This situation is illustrated by figure 1 for a 4  $\mu\text{m}$  thick cell.

Table I cites the results of the top cell current density in micromorph tandem cells with thick LP-CVD ZnO as front contact in dependence of the amorphous i-layer thickness [17]. While this cell design is not entirely comparable to the current experiment, the reported current density of 11.5  $\text{mA}/\text{cm}^2$  in a 350 nm thick top cell of an n-i-p tandem on Asahi U substrate [15] suggests an overall comparable light trapping environment. Table I makes clear that current matching at 12.5  $\text{mA}/\text{cm}^2$  would require unrealistically thick top cells. Taking into account the stabilized values, matching appears impossible.

**Table I:** Current density of the top cells in micromorph tandem cells (identical bottom cells, deposited on hot silver substrate) [17].

Top cell thickness [nm]	Initial current density [ $\text{mA}/\text{cm}^2$ ]	Stabilized current density [ $\text{mA}/\text{cm}^2$ ]
160	9.1	8.7
220	9.5	8.9
300	10.7	10.3
400	11.8	10.6
600	12.1	9.9

#### 3.3 Intermediate reflectors

In order to enhance the photocurrent in the top cell, weakly absorbed light must be prevented from entering the thick bottom cell. This can be achieved by reflection at an additional layer between the bottom and the top cell. Ideally such a layer should be non-absorbing and

conducting, for example, a thin film of a transparent conducting oxide. The amount of reflectivity is related to the contrast in the reflective indices, and the conductivity can be tuned by doping.

For a flattened out geometry like the one shown in figure 1, interference effects can be employed to achieve spectral selectivity; using a intermediate layer thickness  $d = 80$  nm and a material with a refractive index  $n \approx 2$ , enhanced reflection may be expected for a design wavelength of  $\lambda_d = 4n \cdot d \approx 640$  nm. The interference condition does not hold for shorter and longer wavelengths, thus near IR light is transmitted into the bottom cell as desired (visible light is readily absorbed in the top cell and will not see the intermediate reflector).

Using an intermediate reflector of about 100 nm thickness, the top cell current for the 200 nm thick cell shown in table I could be increased from 9.5 to 10.2 mA/cm<sup>2</sup> [13]. This value is consistent with flat solar cells of similar thickness where a second pass through the amorphous absorber layer is established with a reflective back contact metallization. However, even with a second pass the required top cell current would require an unrealistic absorber layer thickness.

The way for further improvement becomes clear when looking into the historical development of amorphous solar cells. In early cells with flat interfaces, a certain improvement was achieved by replacing poor reflectors like molybdenum or chromium with better ones like aluminium or silver [18, 19]. However, major advance in cell efficiencies was only achieved by the introduction of light scattering textures. Consequently, we have to replace the nominally flat intermediate reflector by a film that does not only reflect, but also scatter the weakly absorbed light.

This situation is illustrated in figure 2 by the arrow which represents light that is weakly absorbed in the top cell, e.g. around 700 nm. Without IR, it passes directly into the bottom cell where it is absorbed in the thick microcrystalline film. With flattened interfaces and a thin IR, a part is reflected back into the top cell for a second pass. With a textured IR, there is reflection and scattering with the chance of light trapping into top cell. From an optics point of view, trapping is facilitated by the embedding of a high index material between two low index materials, essentially a classic waveguide situation.

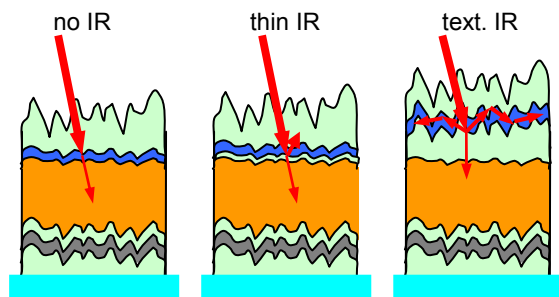
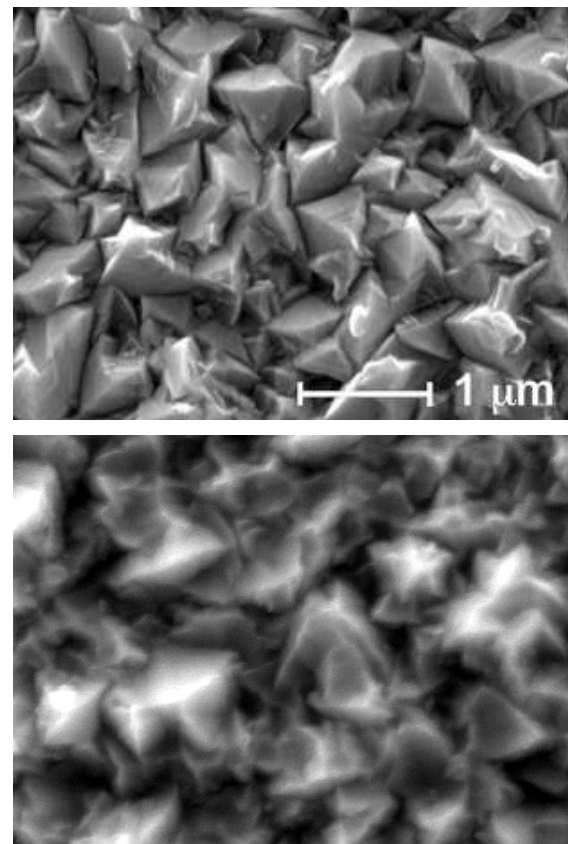


**Figure 2:** Illustration of intermediate reflector concepts in n-i-p micromorph tandem cells. From bottom to top, the layer stack consists of glass/text. SnO<sub>2</sub>/Ag/ZnO/ $\mu$ c-Si cell/ X \a-Si top cell/text. ZnO front contact. Here, X represents the intermediate reflector which is, from left to right, either absent, thin, or thick and textured.

The material of choice for the intermediate reflector is doped ZnO which is conducting and transparent; more

importantly, its low refractive index compared to silicon yields sufficient reflection. The original publication suggested the use of sputtered ZnO which is an ex-situ material [16]. More recently also in-situ materials like phosphorous doped SiO<sub>x</sub> were employed successfully [20]. Commonly these films were intended to work on the basis of their index contrast to silicon and by interference. The latter requires a thickness between 80 and 100 nm which means that these films are essentially flat or reproduce the texture of the underlying cell. In the case of p-i-n cells this concept has been highly successful, but the moderate gain from 9.5 to 10.2 mA/cm<sup>2</sup> in the shown cells suggests that the concept is less applicable n-i-p cells where the back reflector structure is flattened out by the bottom cell. A recent study clearly showed that efficient light trapping requires textures at the front and at the back interface [21, 22].

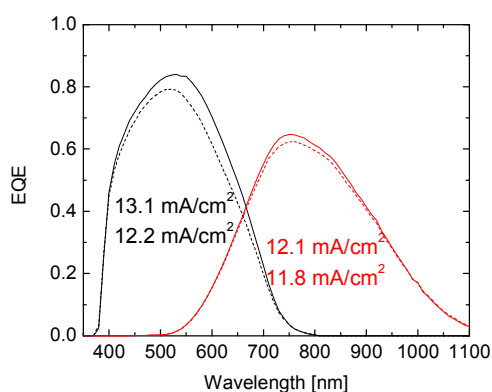
ZnO deposited by LP-CVD is a material that develops suitable interface texture for amorphous cells, it complies also with the other requirements of the intermediate reflector and can be deposited at high rate (typically 3 nm/sec). Figure 3 compares the surface morphology of 1.8  $\mu$ m thick LP-CVD ZnO films grown on flat glass and on a microcrystalline cell. Regardless of the underlying texture, the preferential growth of low-energy surface facets results in the formation of a pyramidal texture which is well suited for amorphous solar cells. The feature size of the texture is controlled by the overall thickness of the film, but depends little on the underlying interface.



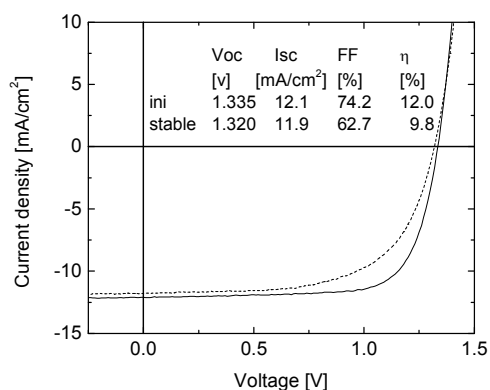
**Figure 3:** Surface morphology of a 1.8  $\mu$ m thick LP-CVD ZnO film, grown on glass (top) and on a microcrystalline bottom cell (bottom). Image size approximately 4 x 3  $\mu$ m<sup>2</sup>.

Figure 4 shows that the use of textured LP-CVD ZnO as intermediate reflector boosts the current density in a 200 nm thick top cell to over 13 mA/cm<sup>2</sup>. The stabilized values show a moderate loss of 7%. While the resulting stabilized current density is in line with the current design goal, higher initial values and reduced degradation are desired; with thicker bottom cells and novel back reflector structures, bottom cell currents higher than 28 mA/cm<sup>2</sup> have already been demonstrated [14].

The j-V curves shown in figure 5 reveal an almost stable Voc, but a rather substantial loss in FF. The high value of the initial FF is very likely related to the current mismatch, but after degradation the tandem is almost matched, and the saturation into the series resistance is not yet reached in the shown range of voltages. Thus the stabilized value of 62.7% indicates that there is an issue with the charge transport. Future development will include an investigation of different hydrogen/silane dilution ratios for the amorphous top cell.



**Figure 4:** External quantum efficiency of a micromorph tandem cell in initial (full lines) and stabilized state (dashed lines).



**Figure 5:** Current voltage characteristics of the micromorph tandem cell in initial (full lines) and stabilized state (dashed lines).

#### 4 SUMMARY AND OUTLOOK

We reported on the introduction of a textured intermediate reflector for micromorph tandem cells in the n-i-p configuration. This concept decouples the light scattering of the two sub-cells, permitting to design two completely independent interface textures that are tailored to the respective requirements of bottom- and top cell. The shown intermediate reflector concept is suitable

for light confinement in the top cell, resulting in current densities above 13 mA/cm<sup>2</sup>. We consider the shown experiments and the stabilized efficiency close to 10% as successful proof of concept at this time; future work must address vital aspects like reduced degradation, the incorporation of improved textures for better IR response in thinner bottom cells, and embossing of such back reflector textures into flexible substrates.

#### 5 ACKNOWLEDGEMENTS

We acknowledge funding from the Swiss Federal Office for Energy (OFEN) under grant No. 101191 and the New Energy and Industrial Technology Development Organization (NEDO), Japan.

#### 6 REFERENCES

- [1] A. Banerjee and S. Guha, *Journal of Applied Physics*, 1991. **69**(2), p. 1030-1035.
- [2] S. Begnali, et al. in *Proc. 24th European PVSEC*. 2009. Hamburg, p. 3BO.9.3.
- [3] K. Katsuma, et al. in *Proc. 22nd European PVSEC*. 2007. Milan, p. 1831.
- [4] E. Yablonovitch and G.D. Cody, *Electron Devices, IEEE Transactions on*, 1982. **29**(2), p. 300-305.
- [5] M. Kambe, et al. in *Proc. 3rd World PVSEC*. 2003. Osaka, p. 1812-1815.
- [6] S. Faÿ, et al., *Solar Energy Materials and Solar Cells*, 2005. **86**(3), p. 385-397.
- [7] O. Kluth, et al., *Thin Solid Films*, 1999. **351**(1-2), p. 247-253.
- [8] M. Fonrodona, et al., *Solar Energy Materials and Solar Cells*, 2005. **89**(1), p. 37-47.
- [9] K. Söderström, et al., accepted for application in *Progress in Photovoltaics: Research and Applications*, 2010.
- [10] K. Söderström, et al. in *Proc. this conference*.
- [11] H. Sai, et al., *Applied Physics Letters*, 2008. **93**, p. 143501.
- [12] T. Söderström, et al., *Journal of Applied Physics*, 2008. **103**(11), p. 114509-114509.
- [13] T. Söderström, et al., *Applied Physics Letters*, 2009. **94**, p. 063501.
- [14] H. Sai and M. Kondo, *Journal of Applied Physics*, 2009. **105**, p. 094511.
- [15] H. Sai and M. Kondo, accepted for publication in *Solar Energy Materials and Solar Cells*, 2010.
- [16] D. Fischer, et al. in *Proc. 25th IEEE PVSC*. 1996. Washington D. C., p. 1053-1056.
- [17] T. Söderström, et al. in *Proc. SPIE Conference*. 2010. San Diego.
- [18] H.W. Deckman, et al., *Applied Physics Letters*, 1983. **42**(11), p. 968-970.
- [19] J. Morris, et al., *Journal of Applied Physics*, 1990. **67**, p. 1079.
- [20] P. Buehlmann, et al., *Applied Physics Letters*, 2007. **91**(14), p. 143505.
- [21] H. Sai and M. Kondo. in *Proc. 35th IEEE PVSC*. 2010. Honolulu.
- [22] H. Sai, H. Jia, and M. Kondo, *Journal of Applied Physics*, 2010. **108**, p. 044505.